JOURNAL OF AGRICULTURAL AND FOOD CHEMISTRY

Article

pubs.acs.org/JAFC

Bioevaluation of Human Serum Albumin−Hesperidin Bioconjugate: Insight into Protein Vector Function and Conformation

Fei Ding,[†,§] Jian-Xiong Diao,[‡] Ye Sun,[†] and Ying Sun*[,‡]

[†]Department of Chemistry, China Agricultural University, Beijing 100193, China

[§]Department of Biological Engineering, Massachusetts Institute of Technology, Cambridge, Massachusetts 02139, United States

[‡]College of Resources and Environmental Sciences, China Agricultural University, Beijing 100193, China

ABSTRACT: Hesperidin is a flavanone glycoside widely available for dietary intake in citrus fruits or citrus fruit derived products; however, exhaustive and reliable data are scarcely available for biological activity when it exerts protective health effects in humans. The principal intent of this work is to check binding domain and structural changes of human serum albumin (HSA), the primary carrier of flavonoids, in blood plasma association with hesperidin by employing molecular modeling, steady state and time-resolved fluorescence, and circular dichroism (CD) methods. From molecular modeling simulations, subdomains IIA and IIIA, which correspond to Sudlow's sites I and II, respectively, were earmarked to possess affinity for hesperidin, but the affinity of site I with flavanone is greater than that of site II. This corroborates the site-specific probe and hydrophobic 8-anilino-1-naphthalenesulfonic acid (ANS) displacement results placing the hesperidin at warfarin−azapropazone and indole−benzodiazepine sites. Steady state and time-resolved fluorescence manifested that static type, due to HSA−hesperidin complex formation (1.941×10^4 M^{-1}), is the operative mechanism for the diminution in the tryptophan (Trp)-214 fluorescence. Moreover, via alterations in three-dimensional fluorescence and CD spectral properties, we can securely draw the conclusion that the polypeptide chain of HSA is partially destabilized after conjugation with hesperidin. We anticipate that this study can provide better knowledge of bioavailability such as absorption, biodistribution, and elimination, of hesperidin in vivo, to facilitate the comprehension of the biological responses to physiologically relevant flavanones.

KEYWORDS: *flavanone glycoside, hesperidin, human serum albumin, protein function, molecular modeling, fluorescence*

INTRODUCTION

Proteins are a miscellaneous and abundant species of biomolecules, comprising >50% of the dry weight of cells. This diversity and abundance mirror the vital role of proteins in nearly all aspects of cell structure and function.[1] However, proteins are dynamic molecules the functions of which almost invariably depend on complexes with other molecules, and these interactions are influenced in physiologically significant ways by sometimes slight and sometimes conspicuous changes in protein conformation.[2] Therefore, knowing specific conformational changes of a protein is an important part of grasping how the protein functions, and the transient essence of protein−ligand conjugations is crucial to life, permitting an organism to respond quickly and reversibly to altering environmental and metabolic circumstances.[1,2]

According to modern notion, practically every ligand present in human blood binds to plasma proteins, and, to a varying extent, these bindings are reversible. This intermolecular interaction produces considerable effect on the pharmacokinetics and pharmacodynamics of many ligands (especially drugs).[3] Protein binding augments ligand solubility in human plasma, meliorating its delivery to the target tissue, which is particularly momentous in the case of low-soluble, hydrophobic chemicals.[4] Ligand conjugation with the protein lessens its toxicity and may fundamentally lengthen the in vivo half-life of a therapeutic compound.[5] All of these outcomes wield sizable effects on the pharmacology of the ligand and, consequently, on its therapeutic activity. It is also generally accepted that only the unbound quantity of drug, habitually referred to as the free concentration, is pharmacologically active and able to pass through cell membranes.[5] The type and magnitude of the protein−drug complexation critically affect the absorption, distribution, metabolism, excretion, and toxicity of a drug. Hence, knowledge of the protein−drug binding is indispensable for the realization of the biochemical consequences of drugs inside the human body, improvement of the efficacy of the formulation and application of proteins in the pharmaceutical and other industries, and the quantitative and qualitative analysis of conformational changes of proteins.[2−6]

Within the plasma proteins, human serum albumin (HSA) is surely the most central transporter for diverse endogenous and exogenous ligands, whereas α_1-acid glycoprotein appears to the degree of 3% of serum albumin to have an inferior whole effect.[4,7] HSA is the most common protein in the bloodstream, accounting for about 60% of the total protein, corresponding to a concentration of 42 mg mL^{-1}, and offering 80% of the osmotic pressure of blood, and has a long history of medical application in colloid replacement treatment.[3,4] The Cochrane Injuries Group Albumin Reviewers[8] conducted a potential excess mortality after human albumin administration in critically ill patients, and some reasonable mechanisms behind the dangerous influence were debated, but varied binding features of human albumin were not involved. The capability of

Received: February 3, 2012
Revised: June 7, 2012
Accepted: June 15, 2012
Published: June 15, 2012

HSA to bind different ligands is greatly dependent on the existence of two well-defined binding regions, namely Sudlow's sites I and II, which are located within specialized pockets in subdomains IIA and IIIA, respectively.[9] These binding sites are often selective, but binding to multiple sites on HSA has also been recognized.[4] As we have said, the ligand-binding peculiarities of protein and its amount in the human body link the protein intimately to the ADMET problem, but these specific molecular interactions are decisive in keeping the high extent of order in a living system, and specific structural alterations are also usually necessary to a protein's function; thus, detailed information concerning binding region and ligand-induced conformational changes of protein are pivotal to understanding conjugations in the biological systems and processes.[10]

Polyphenols occur as secondary metabolites and are considerably dispersed throughout the plant kingdom; many appear in foods and beverages, for example, black tea, aged red wine, coffee, and cocoa.[11] Flavonoids are a chief group of natural polyphenols, and their structures are constituted by 15 carbons, with two aromatic rings linked by a 3-carbon bridge, thence $C_6-C_3-C_6$.[12] These compounds are normally discovered in the form of glycosides in foods of plant origin, especially in vegetables, beverages, and citrus fruits. The pioneer Dr. Albert Szent-Györgyi, who won the Nobel Prize in Physiology or Medicine in 1937, was the first to report the biological activity of flavonoids on capillary fragility associated with scurvy.[13] Hesperidin, a member of the flavanone glycoside of flavonoids (structure shown in Figure 1), is a plentiful and

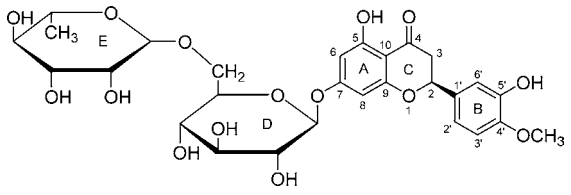

Figure 1. Molecular structure of hesperidin.

inexpensive byproduct of citrus cultivation.[14] So far, specific scientific exertions have evidenced that hesperidin encompasses a variety of pharmacological actions, including effects on the vascular system, anti-inflammatory actions, effects on enzymes, antimicrobial activity, antifertility activity, anticarcinogenic activity, platelet and cell aggregation inhibition, ultraviolet protecting activity, miscellaneous effects, etc.[12,15−17] Moreover, Hitzenberger[18] considers that hesperidin and diosmin displayed an excellent tolerability and, consequently, are usually utilized in combination with therapeutic control of venous diseases. Clinical trials have certified the deficiency of hesperidin in the diet connected with abnormal capillary leakiness as well as pain in the extremities inducing aches, weakness, and night-time leg cramps, and no signs of toxicity have been ascertained with the normal intake of this polyphenolic compound.[12] After administration of 500 mg of hesperidin in water and equivalent amounts of grapefruit and orange juice to healthy white males (human volunteers), 25 years of age, absorption from the gastrointestinal tract was observed but cumulative urinary recovery denoted low bioavailability (<25%).[19] However, more excitingly, Dangles et al.[20] clearly deemed that the bioavailability of flavonoids depends on how they are distributed and transported in different tissues, and it has been proved that a plasma protein, HSA, is the major vector of flavonoids in blood.

Flavonoids' complexation with proteins, especially serum albumins, have been numerously examined in solution by microcalorimetry, fluorescence, nuclear magnetic resonance, ultraviolet−visible (UV−vis) absorption, enzyme inhibition, circular dichroism (CD), high-performance liquid chromatography, Fourier transform infrared spectoscopy (FT-IR), and capillary electrophoresis.[20−30] For example, Papadopoulou et al.[23] tested four flavonoids (catechin, epicatechin, rutin, and quercetin) interacting with bovine serum albumin (BSA) and characterized the chemical association taking place. Dufour and Dangles[30] studied the binding of structurally different flavonoids to HSA and BSA and stated that flavonoids display moderate affinities for serum albumins, and significant differences in affinity and binding patch are also observed for the highly homologous protein. Soares et al.[25] proved that the structure of the flavonoids has some effect on the binding affinity to BSA and human salivary α-amylase. Very recently, Khan et al.[29] checked four flavanone glucuronides and chalcones complexed with HSA and confirmed that flavanone glucuronides and chalcones are moderate HSA ligands with an affinity of 10^4 M^{-1} and that >90% of flavanone derivatives are bound to HSA in physiological conditions. Unfortunately, the tangibility with regard to hesperidin in vivo activity remains ambiguous, and puzzles in relation to its absorption and bioavailability are yet unresolved. Furthermore, to the best of our knowledge, no previous studies are usable on the binding affinity and binding domain of hesperidin with HSA at the molecular level.

Given the above-mentioned background, the main goal of the current research was to generate more comprehensive information about the noncovalent interaction of hesperidin with HSA, the foremost vehicle protein of hesperidin in human plasma. Detailed analyses of the molecular modeling and steady state fluorescence of the HSA−hesperidin complex and time-resolved fluorescence and CD supplied basic data on the observed association reaction. This information can be helpful when developing new drugs whether the purpose is to exploit its reservoir function or to avert binding to HSA.

EXPERIMENTAL PROCEDURES

Materials. Albumin from human serum (A8763, lyophilized powder, essentially globulin free, ≥99%) and hesperidin (50162) utilized in this study were purchased from Sigma-Aldrich (USA) and used without further purification, and deionized water was produced by a Milli-Q Ultrapure Water Purification System from Millipore (USA). All of the experiments were performed in Tris (0.2 M)-HCl (0.1 M) buffer of pH 7.4, with an ionic strength of 0.1 in the presence of NaCl, except where specified, and the pH was checked with an Orion-350 PerpHecT Advanced Benchtop pH-meter (Thermo Scientific, USA). Dilutions of the HSA stock solution (10 μM) in Tris-HCl buffer were prepared immediately before use, and the concentration of HSA was determined spectrophotometrically using $E_{1\ cm}^{1\%} = 5.3$.[31] All solutions were filtered through a 0.2 μm Millex-LG syringe filter (Millipore, USA), and all other reagents employed were of analytical grade and received from Sigma-Aldrich.

Molecular Modeling. Molecular modeling of the HSA−hesperidin complexation was carried out on an SGI Fuel Workstation. The crystal structure of HSA (entry codes 1H9Z), determined at a resolution 2.5 Å, was retrieved from the Brookhaven Protein Data Bank (http://www.rcsb.org/pdb). After importation into the program Sybyl version 7.3 (http://tripos.com), the protein structure was carefully checked for atom and bond type correctness assignment. Hydrogen atoms were computationally added using the Sybyl Biopolymer and Build/Edit menus. To avoid negative acid/acid interactions and repulsive steric clashes, added hydrogen atoms were

energy minimized with the Powell algorithm with a convergence gradient of 0.5 kcal (mol Å)$^{-1}$ for 1500 cycles; this procedure does not change positions of heavy atoms, and the potential of the three-dimensional structure of HSA was assigned according to the AMBER force field with Kollman all-atom charges. The two-dimensional structure of hesperidin was downloaded from PubChem (http://pubchem.ncbi.nlm.nih.gov), and the initial structure of the molecule was generated by Sybyl 7.3. The geometry of hesperidin was subsequently optimized to minimal energy using the Tripos force field with Gasteiger−Hückel charges; the Surflex−Dock program, which employs an automatic flexible docking algorithm, was applied to calculate the possible conformation of the ligand that binds to the protein, and the conformer with root-mean-square deviation (rmsd) was utilized for further analysis.

Steady State Fluorescence. Steady state fluorescence was collected with a 1.0 cm path length quartz cell using an F-4500 spectrofluorometer (Hitachi, Japan) equipped with a thermostatic bath and a microcomputer. The excitation and emission slits were set at 5.0 nm each, intrinsic fluorescence was obtained by exciting the continuously stirred protein solution at 295 nm to selectively excite the tryptophan (Trp) residue, and the emission spectra were recorded in the wavelength range of 295−450 nm at a scanning speed of 240 nm min^{-1}. The reference sample consisting of the Tris-HCl buffer and hesperidin did not give any fluorescence signal.

Time-Resolved Fluorescence. Time-resolved fluorescence was acquired with an FL920P spectrometer (Edinburgh, U.K.), using the time-correlated single-photon counting system with a hydrogen flash lamp excitation source, in air-equilibrated solution at ambient temperature. The excitation wavelength was 295 nm, and the number of counts gathered in the channel of maximum intensity was 2000. The instrument response function (IRF) was conducted by exploiting Ludox to scatter light at the excitation wavelength. The data were analyzed with a nonlinear least-squares iterative method utilizing Edinburgh tail fit software, and the IRF was deconvoluted from the experimental data. The resolution limit after deconvolution was 0.2 ns. The value of χ^2 (0.9−1.2) and the Durbin−Watson parameter (>1.7), as well as a visual inspection of the residuals, were used to assess how well the calculated decay fit the data. Average fluorescence lifetime (τ) for multiexponential function fittings were from the relationship[32]

$$I(t) = \sum_i A_i \, e^{-t/\tau_i} \tag{1}$$

where τ_i represents fluorescence lifetimes and A_i represents their relative amplitudes, with i variable from 1 to 3.

Site-Specific Ligand. Binding location studies between HSA and hesperidin in the presence of four typical site markers (phenylbutazone, flufenamic acid, digitoxin, and hemin) were executed using the fluorescence titration technique. The concentrations of HSA and site markers were all stabilized at 1.0 μM, and then hesperidin was added to the HSA−site markers mixtures. An excitation wavelength of 295 nm was chosen, and the fluorescence emission data of HSA were registered.

Hydrophobic Probe Displacement. In the first series of experiments, HSA concentration was kept fixed at 1.0 μM, and hesperidin/ANS concentration was varied from 10 to 90 μM; HSA fluorescence was gained (λ_{ex} = 295 nm, λ_{em} = 330 nm). In the second series of experiments, hesperidin was added to solutions of HSA and ANS held in equimolar concentration (1.0 μM), and the concentration of hesperidin was also varied from 10 to 90 μM; the fluorescence of ANS was recorded (λ_{ex} = 370 nm, λ_{em} = 465 nm).

Three-Dimensional Fluorescence. The emission wavelength was obtained between 200 and 500 nm, the initial excitation wavelength was set to 200 nm with increments of 10 nm, the number of scanning curves was 16, and the other scanning parameters were identical to those used for steady state fluorescence as mentioned above.

CD Spectra. Far-UV CD spectra were examined with a Jasco-810 spectropolarimeter (Jasco, Japan), equipped with a microcomputer; the apparatus was sufficiently purged with 99.9% dry nitrogen gas before starting the instrument, and then it was calibrated with d-10-camphorsulfonic acid. All of the CD measurements were picked at 298 K with a PFD-425S Peltier temperature controller attached to a water bath with an accuracy of ±0.1 °C. Each spectrum was scanned with the use of a quartz cuvette of 0.2 cm path length and taken at wavelengths between 200 and 260 nm with 0.1 nm step resolution and averaged over five scans operated at a speed of 20 nm min^{-1} and response time of 1 s. A reference sample containing buffer and hesperidin was subtracted from the CD signal for gauge, and conversion to the Mol. CD ($\Delta\varepsilon$) was implemented with Jasco Standard Analysis Software. The HSA secondary structure was computed using CDSSTR, which counts the different assignments of secondary structures by comparison with CD spectra, obtained from distinct proteins for which high-resolution X-ray diffraction data are available.[33] The program CDSSTR is supplied in the CDPro software package, which is available at http://lamar.colostate.edu/~sreeram/CDPro.

THEORY AND CALCULATION

Principles of Fluorescence Quenching. Fluorescence quenching refers to any process that decreases the fluorescence intensity of a sample. A variety of molecular interactions can result in quenching, such as excited state reactions, molecular rearrangements, energy transfer, ground state complex formation, and collisional quenching. Fluorescence quenching is described by the well-known Stern−Volmer equation:[32]

$$\frac{F_0}{F} = 1 + k_q\tau_0[Q] = 1 + K_{SV}[Q] \tag{2}$$

In this equation F_0 and F are the fluorescence intensities in the absence and presence of quencher, respectively, k_q is the bimolecular quenching constant, τ_0 is the lifetime of the fluorophore in the absence of quencher, [Q] is the concentration of quencher, and K_{SV} is the Stern−Volmer quenching constant. Therefore, eq 2 was applied to determine K_{SV} by linear regression of a plot of F_0/F versus [Q].

Calculation of Association Constant. When ligand molecules bind independently to a set of equivalent sites on a macromolecule, the equilibrium between free and bound ligand molecules is given by the relationship[34]

$$\log\left(\frac{F_0 - F}{F}\right) = n\log K - n\log\left(\frac{1}{[Q_t] - \frac{F_0 - F}{F_0}[P_t]}\right) \tag{3}$$

where F_0 and F are the fluorescence intensities in the absence and presence of quencher, respectively, K and n are the association constant and the number of binding sites, respectively, and $[Q_t]$ and $[P_t]$ are the total concentration of quencher and protein, respectively. Thus, a plot of $\log(F_0 - F)/F$ against $\log(1/([Q_t]-(F_0 - F)[P_t]/F_0))$ can be used to calculate K and n. The fluorescence intensities were corrected for absorption of the exciting light and reabsorption of the emitted light to decrease the inner filter effect using the relationship[32]

$$F_{cor} = F_{obs} \times e^{A_{ex}+A_{em}/2} \tag{4}$$

where F_{cor} and F_{obs} are the fluorescence intensities corrected and observed, respectively, and A_{ex} and A_{em} are the absorption of the systems at the excitation and emission wavelengths, respectively. The fluorescence intensity utilized in this study is the corrected intensity.

RESULTS

Molecular Modeling. As mentioned previously, the processes that underlie the complexation of small molecules with protein are intricate, being contingent upon the specific

reactions happening at the molecular level. Interactions between ligands and proteins could be regulated, normally by specific interactions with one or more additional ligands. However, these have been thoroughly investigated as a result of their weightiness in the design of novel therapeutic reagents.[35] HSA is a commonly studied carrier protein because its chief structure is well-known and its tertiary structure has been resolved through X-ray crystallography by Carter and He[9] in 1989 and 1992, thereby offering the basis for the study of the location of ligand-binding sites. It is a globular protein consisting of a single peptide chain of 585 amino acids and has a molecular weight of 66.5 kDa. HSA is constituted by three homologous α-helical domains (I, II, and III), and each domain contains 10 helices, divided into 6-helix and 4-helix subdomains (named A and B) stabilized by 17 disulfide bonds, 1 free thiol (Cys-34) in domain I, and a single Trp residue in position 214 in subdomain IIA.[2−4] Crystallographic data have shown that the binding regions for many various ligands are localized within subdomain IIA or IIIA of the protein molecule; according to Sudlow's nomenclature, these binding domains correspond to sites I and II, respectively.[9] To illuminate the hesperidin binding domain on the protein, we first used computer-aided molecular modeling simulations to inspect and analyze the binding interaction of HSA with hesperidin. The best docking energy result is shown in Figure 2; as can be seen, the hesperidin binding site is situated within subdomains IIA and IIIA, but the affinity of hesperidin with the former is superior, compared with the latter.

In subdomain IIA (ΔG° = −24.82 kJ mol^{-1}), the hydrogen atom of the hydroxyl group in the E- and D-rings and the oxygen atom of the 5-hydroxyl group in the A-ring can make hydrogen bonds with the oxygen atom of the carbonyl group in Arg-257, the nitrogen atom of the heterocyclic ring in His-242, and two hydrogen atoms of amino groups in Arg-218; the bond lengths are 2.626, 1.917, 2.324, and 2.257 Å, respectively. On the basis of surface modification of hesperidin and amino acids composed of subdomain IIA, we can perceive a hydrophobic region at the entrance of subdomain IIA constituted by Phe-211, Trp-214, etc., the hydrophobic group of hesperidin toward the patch, which indicated that hydrophobic interaction was playing an important role between them. Furthermore, the molecular distance between the center of the benzene ring in Trp-214 and the core of A- and B-rings in hesperidin is 5.785 and 5.065 Å, respectively, which illustrated the existence of significant perpendicular $\pi-\pi$ interactions between HSA and hesperidin.

While for subdomain IIIA (ΔG° = −21.34 kJ mol^{-1}), the oxygen atom of 5-hydroxyl group in A-ring, the hydrogen atom of 5′-hydroxyl group in B-ring, and oxygen atom of 4-carbonyl group in C-ring can form hydrogen bonds with two hydrogen atoms of amino group in Lys-414, two hydrogen atoms of hydroxyl group in Tyr-411, and oxygen atom of carbonyl group in Leu-430, their bond lengths, respectively, are 1.913, 2.253, 2.658, 2.740, and 1.884 Å. Hesperidin and subdomain IIIA were also surface modified, and it was found that the hydrophobic group of hesperidin appeared toward the hydrophobic region at the mouth of subdomain IIIA, which is composed by a long carbon chain in Leu-430, Leu-457, Tyr-452, etc.; this result suggests the presence of weak hydrophobic interaction between HSA and hesperidin. In addition, the perpendicular molecular distance between the nucleus of the benzene ring in Tyr-411 and Phe-403 and the kernel of the A- and B-rings in the hesperidin molecule is 6.867 and 5.639 Å; the parallel molecular distance between the heart of the benzene ring and the center of the B-ring in flavanone is 8.517 Å, so enunciating that $\pi-\pi$ interactions also operated between HSA and hesperidin.

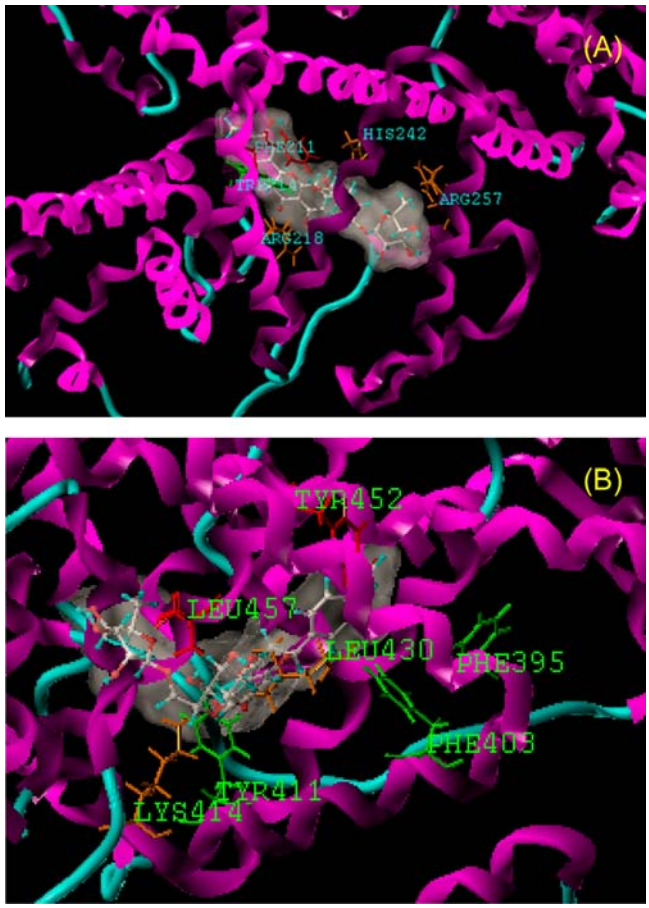

Figure 2. Molecular modeling of hesperidin docked to HSA. Panels A and B depict the amino acid residues involved in binding of hesperidin. The ball-and-stick model indicates hesperidin molecule, colored as per the atoms and possessing white surface of van der Waals radius. The crucial amino acid residues around hesperidin are displayed in stick model; orange color stick model denotes hydrogen bonds between Arg-218, His-242, and Arg-257 residues (A) and between Tyr-411, Lys-414, and Leu-430 residues (B) and hesperidin; red color stick model states hydrophobic interaction between the Phe-211 and Trp-214 residues (A) and Leu-430, Tyr-452, and Leu-457 residues (B) and hesperidin; green color stick model expresses $\pi-\pi$ interactions between the Trp-214 (A) and Phe-395, Phe-403, and Tyr-411 residues (B) and hesperidin.

Considering the molecular modeling simulations described above, it seemed sensible to realize that the dietary flavanone hesperidin was perched on site I (major) and site II (minor), corresponding to subdomains IIA and IIIA, respectively. The overriding driving forces in the HSA−hesperidin conjugation are hydrogen bonds and hydrophobic interactions; perpendicular and parallel $\pi-\pi$ interactions are also not excluded. Additionally, HSA spatial structure was deranged by hesperidin with a partial protein destabilizing. The data displayed in solution experiments recounted below, as derived from steady state and time-resolved fluorescence, site-specific ligand displacement, three-dimensional fluorescence, and CD techniques, were applied to substantiate upper molecular modeling supposition.

Fluorescence Emission of Trp in HSA. Of the several existing methods, fluorescence is largely utilized for checking drug binding to protein or other receptors. Besides its rapidity, accuracy, sensitivity, and convenience of handling, fluorescence allows noninvasive detection of solute at low concentrations under physiological conditions.[36] Because aromatic amino acid residues in proteins have intrinsic fluorescence, assessment of the quenching of the fluorescence by a ligand can unveil the accessibility of this ligand to the HSA fluorophore, assist understanding of the association and mechanism, and proffer an inkling to the character of the binding event.[32] Figure 3 displays

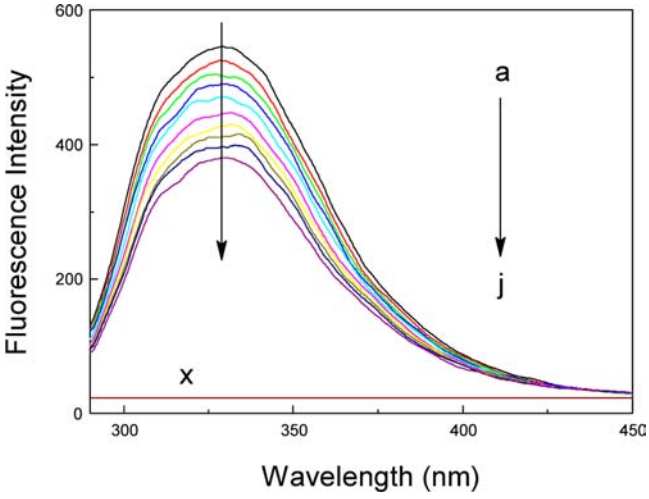

Figure 3. Steady state fluorescence of HSA with various amounts of hesperidin (pH 7.4, T = 298 K): (a) 1.0 μM HSA; (b–j) 1.0 μM HSA in the presence of 10, 20, 30, 40, 50, 60, 70, 80, or 90 μM hesperidin; (x) 90 μM hesperidin only.

the steady state fluorescence for quenching of Trp-214 in HSA at pH 7.4 with different amounts of hesperidin. Evidently, HSA exhibited a strong fluorescence emission at 330 nm following an excitation at 295 nm, and the increment of hesperidin fomented a continuing reduction of the fluorescence signal. Under the experimental conditions, hesperidin revealed no fluorescence emission in the range of 295–450 nm, which did not affect HSA intrinsic Trp-214 fluorescence. This surveillance hinted that there was reaction between HSA and hesperidin, and hesperidin located in the subdomain where Trp-214 situated within or near the sole fluorophore.[37] To discern the fluorescence quenching mechanism, Stern–Volmer eq 2 was used for data analysis, and the corresponding results fitted from Stern–Volmer plots (Figure 4) are summarized in Table 1. The outcomes proclaim obviously that the Stern–Volmer quenching constant K_{SV} is the counter correlated with temperature, and the value of k_q is 10 times higher than the maximum value for diffusion-controlled quenching in water ($\sim 10^{10}$ M^{-1} s^{-1}), signifying the probable quenching mechanism for HSA fluorescence by hesperidin is a static type.[32,34]

Time-Resolved Fluorescence. Albeit static and dynamic quenching may be differentiated by their diverging dependence on temperature and viscosity, according to the theory of Lakowicz,[32] fluorescence quenching is preferably acquired by time-resolved fluorescence measurements, which can distinguish between static and dynamic processes immediately. Accordingly, the representative fluorescence decay pictures of HSA at various molar ratios of hesperidin in Tris-HCl buffer, pH 7.4, are expressed in Figure 5, and the fluorescence lifetimes

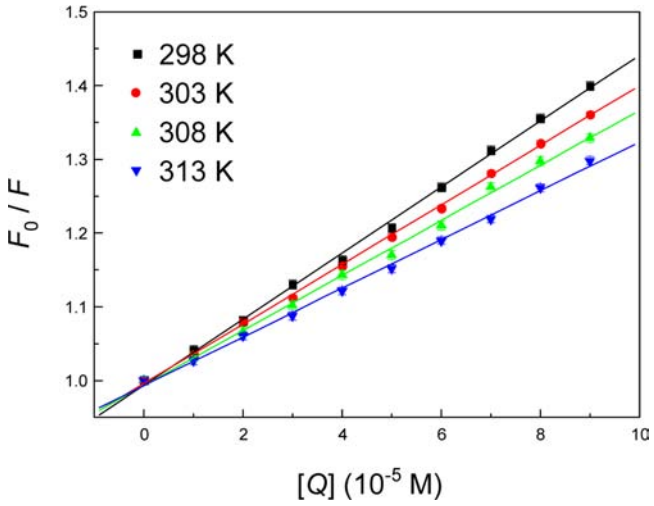

Figure 4. Stern–Volmer plots describing fluorescence quenching of HSA in the presence of different concentrations of hesperidin. Each data point represents the mean of three independent observations ± SD ranging from 0.35 to 0.62%.

Table 1. Stern–Volmer Quenching Constants for the Association of HSA with Hesperidin at Different Temperatures

T (K)	K_{SV}[a] (× 10^3 M^{-1})	k_q (× 10^{11} M^{-1} s^{-1})	R[b]
298	4.478 ± 0.006	8.417 ± 0.006	0.9991
303	4.038 ± 0.003	7.59 ± 0.003	0.9996
308	3.729 ± 0.006	7.009 ± 0.006	0.9987
313	3.305 ± 0.005	6.212 ± 0.005	0.9987

[a]The mean value of three independent experiments with standard deviation (SD) ±0.35–0.62%. [b]R is the correlation coefficient.

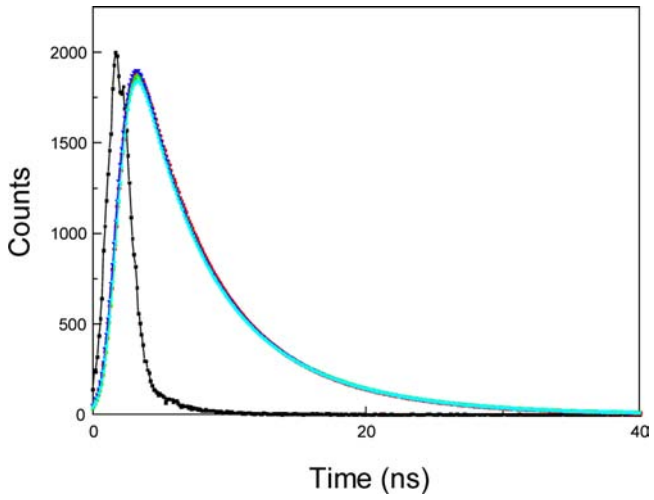

Figure 5. Time-resolved fluorescence decays of HSA in Tris-HCl buffer, pH 7.4. c(HSA) = 10 μM; c(hesperidin) = 0 (●), 10 (▲), 20 (▼), and 40 (♦) μM. The sharp pattern on the left (■) is the lamp profile.

and their amplitudes are pooled in Table 2. The decay curves fitted well to a biexponential function; the relative fluorescence lifetime is τ_1 = 2.49 ns and τ_2 = 6.59 ns (χ^2 = 1.19) of HSA, whereas in the maximum concentration of hesperidin, the lifetime is τ_1 = 2.55 ns and τ_2 = 6.61 ns (χ^2 = 1.19). As Trp is known to display multiexponential decays, we have not

dx.doi.org/10.1021/jf300424w | J. Agric. Food Chem. 2012, 60, 7218–7228

Table 2. Fluorescence Lifetime of HSA as a Function of the Concentrations of Hesperidin

sample	τ_1[a] (ns)	τ_2 (ns)	A_1	A_2	τ (ns)	χ^2
free HSA	2.49	6.59	0.31	0.69	5.32	1.19
HSA + hesperidin (1:1)	2.44	6.52	0.29	0.71	5.33	1.20
HSA + hesperidin (1:2)	2.85	6.80	0.37	0.63	5.33	1.15
HSA + hesperidin (1:4)	2.55	6.61	0.32	0.68	5.31	1.19

[a]The uncertainty in the values of fluorescence lifetime and amplitude is <5%.

attempted to assign the individual components. Conversely, the average lifetime has been utilized to obtain a qualitative analysis. The average lifetime of HSA did not alter significantly, only from 5.32 to 5.31 ns, at different hesperidin concentrations, thus indicating that fluorescence quenching is an essentially static mechanism.[38] This observation also coincides with our inference based on steady state fluorescence data that the quenching is static in nature, and the hesperidin molecule binds in the vicinity of Trp-214. For further validation of this assertion we have studied the competitive binding of the hesperidin with some archetypal fluorescent ligands, which are known to bind to specific regions in HSA, and the outcomes of these studies are detailed in the next section.

Identification of Binding Domain on HSA. To ascertain hesperidin binding location on the HSA, competitive binding experiments have been carried out, using probes that specifically bind to a known site or domain. As has been argued, HSA is known to contain two chief binding sites for ligands, called Sudlow's sites I and II, as well as several minor binding sites.[2−4] Site I is known as the warfarin−azapropazone site and is formed as a pocket in subdomain IIA; the characteristic feature of this site is the binding of the ligand, which is a bulky heterocyclic anion with a negative charge localized in the middle of the molecule.[4] Ligands binding in this site include warfarin, phenylbutazone, valproate, and azapropazone. Site II corresponds to the pocket of subdomain IIIA and is known as the indole−benzodiazepine site; the interior of the cavity is constituted of hydrophobic amino acid residues, and the pocket exterior presented two important amino acid residues (Arg-410 and Tyr-411).[9] Drugs binding to site II are aromatic carboxylic acids with a negatively charged acidic group at the end of the molecule, such as ibuprofen, flufenamic acid, diazepam, and flurbiprofen. Shortly thereafter, Brodersen et al.[39] pointed out that digitoxin binding in HSA is sovereign of Sudlow's site I or II, and perching on what was nominated as site III. In the current experiment, the competitors utilized included phenylbutazone, a characteristic marker for site I, flufenamic acid for site II, digitoxin for site III, and hemin for domain I. On the basis of the plots of eq 3, the association constants were calculated from fluorescence data and found to be $K = (1.941 \pm 0.007) \times 10^4$, $(0.1371 \pm 0.008) \times 10^4$, $(0.5471 \pm 0.012) \times 10^4$, $(1.578 \pm 0.015) \times 10^4$, and $(1.729 \pm 0.015) \times 10^4$ M^{-1} for blank, phenylbutazone, flufenamic acid, digitoxin, and hemin, respectively. The results fitted evinced that the bound HSA−hesperidin complex was most influenced by the addition of phenylbutazone, followed by flufenamic acid; in other words, hesperidin binding to HSA is principally located within subdomains IIA and IIIA and has greater affinity with Sudlow's site I. This corroborates the outcome of molecular modeling simulations placing the hesperidin at subdomains IIA and IIIA and is also in agreement with hydrophobic probe ANS experiments below.

Hydrophobic Probe ANS. The fluorescent probe 8-anilino-1-naphthalenesulfonic acid (ANS), which is sensitive to microenvironmental changes and can serve as a suitable reporter of interaction in the neighborhood of protein Trp residue, thereby has been employed to characterize all of the hydrophobic binding sites of proteins.[40] The aim of executing ANS studies was to further confirm the essence of the hesperidin binding patch in HSA. According to the protocol, binding studies were practiced in the presence of ANS under identical conditions; the relative fluorescence (F/F_0) against ligand concentration ([ligand]) plots is denoted in Figure 6. At

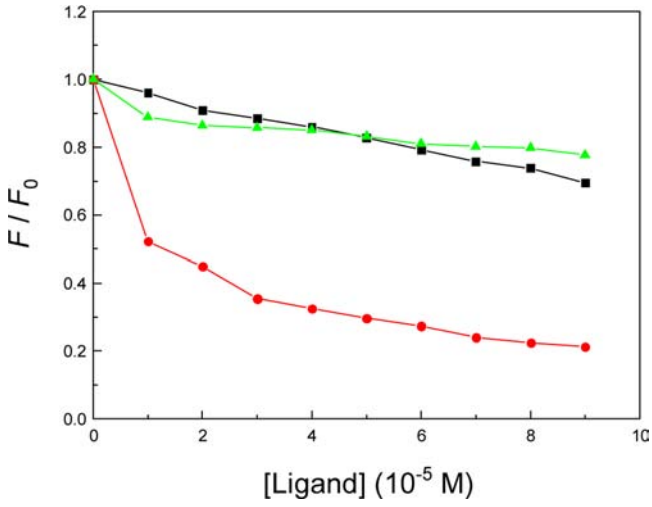

Figure 6. Fluorescence quenching profiles of HSA and HSA−ANS mixture: binding isotherm of hesperidin (■) and ANS (●) induced quenching of HSA fluorescence and quenching of HSA−ANS complex fluorescence by hesperidin (▲); pH 7.4, T = 298 K.

a ligand concentration of 90 μM, both hesperidin and ANS decrease Trp-214 residue fluorescence, but the extent of quenching by hesperidin was much less as compared to ANS; ANS could quench about 78.69%, whereas hesperidin could only diminish about 30.52% of Trp fluorescence. Stryer[41] first reported that the quantum yield of ANS is about 0.002 in aqueous buffer, but near 0.4 when bound to albumin, with almost no contribution from the unbound probe. When hesperidin is added to the HSA−ANS mixture, it can contend for ANS and displace ANS from its binding site; thus, the fluorescence would reduce. As can be seen from Figure 6 about 22.38% of ANS fluorescence has vanished, explaining how hesperidin can compete against ANS for its binding site. Although still partly controversial, consensus exists today that there are four hydrophobic binding sites for ANS associated with HSA, but preferentially at a site in subdomain IIIA.[42] In this context, ANS intensely quenches the fluorescence of HSA, which proves that the binding location for ANS is in this high-affinity site (subdomain IIIA); also, approximately 22.38% displacement of ANS fluorescence attests that hesperidin and ANS share a common site in HSA, that is, Sudlow's site II, but not predominantly.

Three-Dimensional Fluorescence. As set forth, the binding of a protein and ligand is often coupled to a structural change in the protein that makes the binding site more complementary to the ligand, permitting tighter binding, so

dx.doi.org/10.1021/jf300424w | J. Agric. Food Chem. 2012, 60, 7218−7228

conformational alterations of proteins are a factor of biological function. We have utilized three-dimensional fluorescence to detect the structural changes of HSA upon association with hesperidin as alluded to molecular modeling. Figure 7

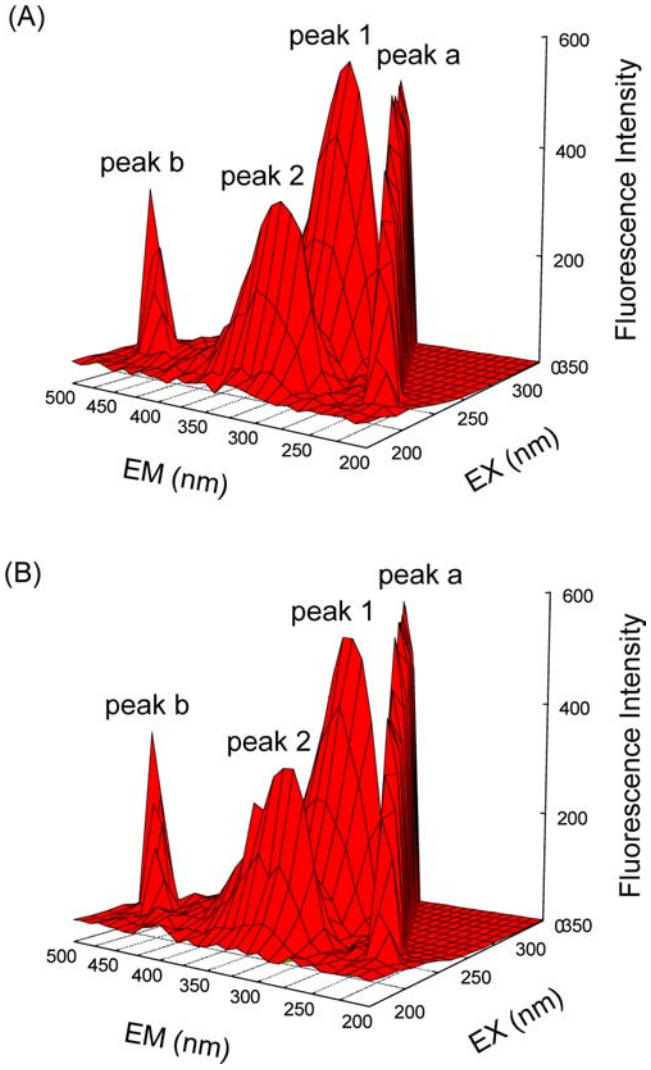

Figure 7. Three-dimensional fluorescence spectra of HSA (A) and the HSA–hesperidin mixture (B): (A) c(HSA) = 1.0 μM, c(hesperidin) = 0; (B) c(HSA) = 1.0 μM, c(hesperidin) = 10 μM; pH 7.4, T = 298 K.

represents the three-dimensional fluorescence of HSA and a HSA–hesperidin complex, and the corresponding parameters are collected in Table 3. Peak a ($\lambda_{ex} = \lambda_{em}$) is the Rayleigh scattering peak, and peak b ($\lambda_{em} = 2\lambda_{ex}$) is the second-order scattering peak. Peak 1 (λ_{ex} = 280.0 nm, λ_{em} = 323.0 nm) mainly exhibits the spectral feature of tyrosine (Tyr) and Trp residues. Because when HSA is excited at 280 nm, it primarily displays the intrinsic fluorescence of Tyr and Trp residues, and the phenylalanine (Phe) residue's fluorescence can be negligible.[32] Besides peak 1, peak 2 (λ_{ex} = 230.0 nm, λ_{em} = 323.0 nm) chiefly signifies the fluorescence spectral behavior of the polypeptide chain backbone structure C═O. The fluorescence of peak 2 decreased after the addition of hesperidin, which implied that the peptide chain structure of HSA was altered, and this supports previous molecular modeling. By comparison with the fluorescence intensity of peaks 1 and 2, in the presence and absence of hesperidin, the intensity ratios of the two peaks were 1:1.06 and 1:1.04, respectively, meaning the adduct of HSA and hesperidin induced the small destabilization of the polypeptide chain of HSA, which increased the exposure of some hydrophobic regions that had been buried before. The structural changes detected via three-dimensional fluorescence are in good conformity with molecular modeling simulations and also coincided with the far-UV CD data below.

Far-UV CD. CD is a powerful analytical approach to study the association of proteins with other ligands and to determine the protein conformation in solution. To quantitatively analyze the secondary structure changes of HSA, the far-UV CD spectra of HSA with various amounts of hesperidin were scanned and secondary structure components calculated on the basis of raw CD data listed in Table 4. The CD curve of HSA displayed two

Table 4. Secondary Structure of HSA Complexes with Hesperidin at pH 7.4 Calculated by CDSSTR Software[a]

	secondary structure components (%)			
sample	α-helix (±1%)	β-sheet (±1%)	turn (±2%)	random (±1%)
free HSA	51.9	7.2	19.9	21.0
HSA + hesperidin (1:2)	48.1	8.2	21.2	22.5
HSA + hesperidin (1:4)	46.7	8.7	21.5	23.1

[a]Each value denotes the average of observations from five separate experiments; curve fitting and data analysis were conducted on each experiment, and SD was computed.

negative bands in the far-UV region at 208 and 222 nm, typical of the α-helical structure of protein.[33] The prudent explanation is that the negative peaks between 208 and 209 nm and between 222 and 223 nm are both contributed by $n\rightarrow\pi^*$ transition for the peptide bond of the α-helix. As shown in Table 4, free HSA has 51.9% α-helix, 7.2% β-sheet, 19.9% turn, and 21% random coil; upon complexation with hesperidin, lessening of α-helix was observed to 46.7% in the HSA–hesperidin complex, whereas increases in β-sheet, turn, and random coil to 8.7, 21.5, and 23.1%, respectively, in the HSA–hesperidin adduct at a molar ratio of HSA to hesperidin of 1:4 were found. The drop of α-helix with an increase in the β-sheet, turn, and random coil revealed that hesperidin bonds with the amino acid residue of the polypeptide chain, and this evokes

Table 3. Three-Dimensional Fluorescence Spectral Characteristic Parameters of HSA and HSA–Hesperidin Complex

	HSA			HSA–hesperidin		
peak	peak position $\lambda_{ex}/\lambda_{em}$ (nm/nm)	Stokes $\Delta\lambda$ (nm)	intensity F	peak position $\lambda_{ex}/\lambda_{em}$ (nm/nm)	Stokes $\Delta\lambda$ (nm)	intensity F
Rayleigh scattering peaks	250/250→350/350	0	297.8→493.1	250/250→350/350	0	302.2→579.7
fluorescence peak 1	280.0/323.0	43.0	548.1	280.0/326.0	46.0	518.3
fluorescence peak 2	230.0/323.0	93.0	325.3	230.0/325.0	95.0	311.4

dx.doi.org/10.1021/jf300424w | J. Agric. Food Chem. 2012, 60, 7218–7228

some degree of protein destabilization.[33,43] All of the above observations and analyses ratified the complexation of hesperidin with HSA initiated spatial structure changes in HSA, which may be correlated with its physiological activity.

DISCUSSION

In human foods, flavanones are found virtually exclusively in fresh or processed forms of citrus fruits and juice; for this reason, the daily intake of hesperidin is mostly dependent on dietary habits. In the United States, the average daily personal consumption of citrus fruits and juices has been evaluated as 68 g, of which 59 g was consumed as juices.[44] The most generally consumed orange juice comprises between 200 and 600 mg of hesperidin and 15−85 mg of narirutin per liter, and a single glass of orange juice may involve 40−140 mg of flavanone glycosides.[45] The solid portions of citrus fruit, especially the albedo (the spongy white tissue on the inside of the rind of citrus fruit) and the membranes separating the segments, have a large flavanone component, and the entire fruit could include up to 5-fold as much as a glass of orange juice.[46] As previously stated, on the basis of results on plasma and urinary concentrations, the bioavailability of hesperidin is restricted. Nielsen et al.[47] plainly affirmed that the bioavailability of hesperidin was adjusted by the enzymatic conversion to hesperetin-7-glucoside, veering the absorption location from the colon to the small intestine. Nevertheless, Gardana et al.[48] put forward that hesperidin uptake occurs not only in the small intestine but also in the large intestine. It is important to understand that human tissues are exposed to flavanones through the blood, which is the lone path via which dietary hesperidin may arrive at tissues and their cells.[12,19,20] As a matter of fact, flavanones are not unrestrained in the blood; for instance, Boulton et al.[49] intelligibly demonstrated that quercetin is widely complexed with healthy normal human plasma proteins (99.4 ± 0.1% for concentrations no less than 15 μM); however, binding to very-low-density lipoproteins is not notable (<5%). This consequence was upheld by Dangles and Dufour,[24] who approved polyphenol−plasma protein conjugations prior to intestinal absorption, and this binding contained flavonoid bioavailability, whereas the biological significance of these flavonoid−protein associations in the area of human nutrition awaits in vivo certification.

All of the experiments clarified herein, for the first time, unmask the binding patch, binding affinity, and structural changes of HSA upon flavanone glycoside hesperidin complexation. Hesperidin located at subdomains IIA and IIIA of HSA, but the affinity of subdomain IIIA to hesperidin was lower than that of subdomain IIA; the affinity difference may be related to the molecular conformation of hesperidin in the two pockets and the key amino acid residues composed of the cavities.[50] Site I is a large and flexible region with respect to site II;[51,52] the molecular conformation of hesperidin was more extended when it bound at site I, and hesperidin can interact directly with consequential amino acid residues in subdomain IIA, such as Trp-214, His-242, and Arg-257, through hydrogen bonds, and hydrophobic and $\pi-\pi$ interactions. Whereas for the two paramount amino acid residues, Arg-410 and Tyr-411, the significant active binding sites of subdomain IIIA, hesperidin reacts only with Tyr-411 by hydrogen bonds and $\pi-\pi$ interactions, and no interaction was observed between hesperidin and the Arg-410 residue. Furthermore, the remarkable thing is that, in most proteins, Arg can reinforce the conjuagation between ligands and peptide chain via producing an annexed site of reaction but does not by itself shape an individual powerful binding site.[53] As a result, the acting forces of hesperidin in subdomain IIA are greater than in subdomain IIIA; that is, the affinity of hesperidin with site I is higher than that with site II.

It is particularly worth noting that HSA holds a unique Trp-214 residue in domain II (loop 4); for the purpose of getting evidence regarding the accessibility of hesperidin to this fluorophore, the fluorescence excitation wavelength was set at 295 nm to selectively excite the Trp residue. In the present work, molecular modeling simulations divulge the binding of hesperidin to HSA mainly located within subdomains IIA (major) and IIIA (minor). This phenomenon was certified by competitive fluorescent ligand binding, which asserted phenylbutazone and flufenamic acid as marker ligands of Sudlow's sites I and II, vying with hesperidin for the two domains. However, the affinity of hesperidin with site II was less than that with site I, which further sustained the results of hydrophobic probe ANS displacement binding. The observations may be unraveled with the fact that subdomains IIA and IIIA share a common interface; Trp-214 plays an imperative structural role in the construction of the subdomain IIA binding region through partaking in an additional hydrophobic interdomain clustering interaction between the IIA and IIIA interface.[4,53] Hesperidin can enter the crevice between helices h1 and h2, underneath which lies the only Trp of HSA. Consequently, this finding provided a good structural ground to explicate the very effective fluorescence quenching of Trp-214 emission in the presence of another ligand, which has an analogous configuration with hesperidin. This binding mode of conjugation also agrees with earlier outcomes for experimental and theoretical methods engaged to examine the molecular interaction of the analgesic and antipyretic drug paracetamol with HSA.[54]

Xie et al.[22] narrated the complexation of hesperetin with HSA in the pH range from 6.4 to 8.4; their results pointed out that the binding affinity for HSA−hesperetin was 8.11×10^4 M^{-1}, the basal binding patch was located on subdomain IIA, and the phenolic hydroxyl groups played an important function for the binding process and the transition of protein secondary structure. In the present case, the affinity of HSA−hesperidin is 1.941×10^4 M^{-1}, smaller than that of the HSA−hesperetin complex; a credible elucidation is that hesperidin is a β-7-rutinoside of hesperetin, the disaccharide segment consisting of one molecule of rhamnose and one of glucose and could take one of the two isomeric forms, rutinose or neohesperidose.[11,12,14] In the hesperidin structure, glucose is attached to hesperetin and rhamnose is appended to the glucose; it is then 3′,5,7-trihydroxy-4′-methoxyflavanone-7-(6-α-L-rhamnopyranosyl-β-D-glucopyranoside or -7-rutinoside). The glycosylation may enlarge the molecular size, polarity, and steric resistance of hesperidin, which declines the binding affinity for HSA; our conclusions are in excellent consonance with the opinion recently put forth by Xiao and Kai.[55] In comparison with other flavonoids,[25−30] for example, tannic acid, (+)-catechin, malvidin-3-glucoside, rutin, luteolin, naringenin, wogonin, and tangeretin, the affinity reckoned for the HSA−hesperidin complex represents weak binding. Molecular modeling also verified that no matter hesperidin binded at IIA or IIIA subdomain of HSA, the hydroxyl groups in the A- and B-rings of hesperidin are all fundamental functional groups, which can react with C═O, N—H, and O—H of amino acid residues, such as Arg, His, Tyr, Lys, and Leu,[56] by making

hydrogen bonds. This is consistent with the prediction using FT-IR spectra in the deuterium oxide buffer,[22] the hydrogen atoms of phenolic hydroxyl groups in the A- and B-rings replaced by deuterium atom, forming −OD group, and the capacity of −OD is lower than that of −OH for creating hydrogen bonds.

Again, according to the equation $\Delta G^\circ = -RT \times \ln K$, we can also calculate the experimental binding energy $\Delta G^\circ = -24.46$ kJ mol^{-1}, which connotes the HSA−hesperidin association process was spontaneous and the formation of the adduct was an exothermic reaction. It is noteworthy that the inherent attraction of flowing hesperidin adducts for HSA should be much less than that of hesperetin itself, but the normal level of serum albumin (∼640 mM) is, in all probability, high enough to tolerate massive conjugation.[20,24] The strength of binding to HSA could have importance for the speed of clearance of hesperidin and for their transport to cells and tissues. As seen above, merely the free pattern of drug exerts pharmacological action owing to its capability to pass the membranes and to complex with receptors. As the unbound drug departs the circulatory system and permeates tissues or experiences excretion, the disassociation of the protein−drug coordination must operate quickly to maintain the balance between the free and complexed drug concentrations.[57−59] Still, fluctuation in regional pH at particular sites could engender structural alterations in HSA, which bring about dissociation of the HSA−hesperidin conjugate. Hesperidin induced disturbance of the HSA spatial structure by a predominant shrinkage of α-helix structure from 51.9% in the free protein to 46.7% in the HSA−hesperidin complex, leading to a partial protein disordering. The stability of the HSA−hesperidin adduct may be due to the presence of hydrogen bonds and hydrophobic and $\pi-\pi$ interactions; hydrogen bonds also resulted in the rearrangement of the polypeptide chain network and, as a consequence, abatement of the HSA α-helix.

To sum up, our task endows salutary quantitative data on the location, affinity, and spatial structural changes of hesperidin to the dominant vector of flavanone in human plasma, HSA by mingling computational and experimental techniques of analysis. The results depicted hesperidin is associated in both subdomains IIA (major) and IIIA (minor) of HSA, where explicit interactions, for example, hydrogen bonds and hydrophobic and $\pi-\pi$ interactions, take place. Steady state and time-resolved fluorescence measurements have insinuated that hesperidin binding to HSA is static type, with a low affinity of 10^4 M^{-1}. The HSA spatial structure was somewhat destabilized by hesperidin association with a loss of α-helix and an increase of β-sheet, turn, and random coil structures. Even though it is popularly believed that hesperidin may be hydrolyzed by colonic microflora before its absorption, whereas hesperetin aglycone, as well as the monosaccharide hesperetin 7-*O*-glucoside, could previously be absorbed in the gastrointestinal tract, it occurs just at special positions.[60] Does the complexed hesperidin or its unbound form possess particular biological activity? Dangles et al.[20,61] exemplified the 1,2-dihydroxybenzene fragment of bovine serum albumin-bound quercetin and quercetin derivatives remains approachable to oxidizers such as sodium periodate. If this crucial structural unit of quercetin is also available to free radicals, quercetin may exercise its antioxidant activity even when it is complexed with bovine serum albumin. The biological activities of flavanones are of course not restricted simply to their antioxidant ability; as a consequence, conjugation to serum albumins could possess significant influence. The complexation of hesperidin with HSA specified here, therefore, can be utilized as a biologically pertinent model for appraising the physiologically germane coordination complexes in in vitro investigations of flavanone properties, because characterization of the physiological flavonoid conjugates is an indispensable precondition to comprehending the function of dietary flavonoids in human health.

AUTHOR INFORMATION

Corresponding Author

*Phone/fax: +86-10-62734676. E-mail: sunying@cau.edu.cn.

Funding

This work was accomplished under the auspices of the National Natural Science Foundation of China (No. 31171693).

Notes

The authors declare no competing financial interest.

ACKNOWLEDGMENTS

We are indebted to Professor Ulrich Kragh-Hansen of the Department of Medical Biochemistry, University of Aarhus, for the priceless gift of his doctoral dissertation. We appreciate Dr. Xiu-Nan Li of Institute of Process Engineering, Chinese Academy of Sciences, for his continual support during the circular dichroism measurements. We are grateful to Wei Liu for her constructive assistance in language correction and manuscript refinement. We thank the reviewers of this paper for their invaluable suggestions.

ABBREVIATIONS USED

HSA, human serum albumin; BSA, bovine serum albumin; Arg, arginine; Cys, cysteine; His, histidine; Leu, leucine; Lys, lysine; Phe, phenylalanine; Trp, tryptophan; Tyr, tyrosine; ANS, 8-anilino-1-naphthalenesulfonic acid; Tris, tris(hydroxymethyl)-aminomethane; ADMET, absorption, distribution, metabolism, excretion, and toxicity; CD, circular dichroism; FT-IR, Fourier transform infrared spectroscopy; IRF, instrument response function; UV−vis, ultraviolet−visible spectroscopy; R, correlation coefficient; rmsd, root-mean-square deviation; SD, standard deviation.

REFERENCES

(1) Murray, R. K.; Granner, D. K.; Mayes, P. A.; Rodwell, V. W. *Harper's Illustrated Biochemistry*, 26th ed.; McGraw-Hill: New York, 2003.

(2) Curry, S. Lessons from the crystallographic analysis of small molecule binding to human serum albumin. *Drug Metab. Pharmacokinet.* **2009**, *24*, 342−357.

(3) Ahmed-Ouameur, A.; Diamantoglou, S.; Sedaghat-Herati, M. R.; Nafisi, S.; Carpentier, R.; Tajmir-Riahi, H. A. The effects of drug complexation on the stability and conformation of human serum albumin: protein unfolding. *Cell Biochem. Biophys.* **2006**, *45*, 203−213.

(4) Peters, T., Jr. *All about Albumin: Biochemistry, Genetics, and Medical Applications*; Academic Press: San Diego, CA, 1995.

(5) Flarakos, J.; Morand, K. L.; Vouros, P. High-throughput solution-based medicinal library screening against human serum albumin. *Anal. Chem.* **2005**, *77*, 1345−1353.

(6) Beauchemin, R.; N'soukpoé-Kossi, C. N.; Thomas, T. J.; Thomas, T.; Carpentier, R.; Tajmir-Riahi, H. A. Polyamine analogues bind human serum albumin. *Biomacromolecules* **2007**, *8*, 3177−3183.

(7) Pérez-Ruiz, R.; Bueno, C. J.; Jiménez, M. C.; Miranda, M. A. In situ transient absorption spectroscopy to assess competition between serum albumin and α-1-acid glycoprotein for drug transport. *J. Phys. Chem. Lett.* **2010**, *1*, 829−833.

(8) Cochrane Injuries Group Albumin Reviewers.. Human albumin administration in critically ill patients: systematic review of randomised controlled trials. *BMJ* **1998**, *317*, 235−240.
(9) Carter, D. C. Crystallographic survey of albumin drug interaction and preliminary applications in cancer chemotherapy. In *Burger's Medicinal Chemistry, Drug Discovery, and Development*, 17th ed.; Abraham, D. J., Rotella, D. P., Eds.; Wiley: Hoboken, NJ, 2010; p 437.
(10) Bekard, I. B.; Asimakis, P.; Teoh, C. L.; Ryan, T.; Howlett, G. J.; Bertolini, J.; Dunstan, D. E. Bovine serum albumin unfolds in Couette flow. *Soft Matter* **2012**, *8*, 385−389.
(11) Crozier, A.; Jaganath, I. B.; Clifford, M. N. Dietary phenolics: chemistry, bioavailability and effects on health. *Nat. Prod. Rep.* **2009**, *26*, 1001−1043.
(12) Garg, A.; Garg, S.; Zaneveld, L. J. D.; Singla, A. K. Chemistry and pharmacology of the citrus bioflavonoid hesperidin. *Phytother. Res.* **2001**, *15*, 655−669.
(13) Rusznyák, S.; Szent-Györgyi, A. Vitamin P: Flavonols as vitamins. *Nature* **1936**, *138*, 27.
(14) Jaganath, I. B.; Crozier, A. Dietary flavonoids and phenolic compounds. In *Plant Phenolics and Human Health: Biochemistry, Nutrition, and Pharmacology*; Fraga, C. G., Ed.; Wiley: Hoboken, NJ, 2010; p 1.
(15) Pan, M.-H.; Lai, C.-S.; Ho, C.-T. Anti-inflammatory activity of natural dietary flavonoids. *Food Funct.* **2010**, *1*, 15−31.
(16) Hwang, S.-L.; Shih, P.-H.; Yen, G.-C. Neuroprotective effects of citrus flavonoids. *J. Agric. Food Chem.* **2012**, *60*, 877−885.
(17) Chanet, A.; Milenkovic, D.; Manach, C.; Mazur, A.; Morand, C. Citrus flavanones: what is their role in cardiovascular protection? *J. Agric. Food Chem.* **2012**, DOI: 10.1021/jf300669s.
(18) Hitzenberger, G. Therapeutic effectiveness of flavonoids illustrated by daflon 500 mg. *Wien. Med. Wochenschr.* **1997**, *147*, 409−412.
(19) Ameer, B.; Weintraub, R. A.; Johnson, J. V.; Yost, R. A.; Rouseff, R. L. Flavanone absorption after naringin, hesperidin, and citrus administration. *Clin. Pharmacol. Ther.* **1996**, *60*, 34−40.
(20) Dangles, O.; Dufour, C.; Manach, C.; Morand, C.; Remesy, C. Binding of flavonoids to plasma proteins. *Methods Enzymol.* **2001**, *335*, 319−333.
(21) Papadopoulou, A.; Frazier, R. A. Characterization of protein-polyphenol interactions. *Trends Food Sci. Technol.* **2004**, *15*, 186−190.
(22) Xie, M.-X.; Xu, X.-Y.; Wang, Y.-D. Interaction between hesperetin and human serum albumin revealed by spectroscopic methods. *Biochim. Biophys. Acta−Gen. Subj.* **2005**, *1724*, 215−224.
(23) Papadopoulou, A.; Green, R. J.; Frazier, R. A. Interaction of flavonoids with bovine serum albumin: a fluorescence quenching study. *J. Agric. Food Chem.* **2005**, *53*, 158−163.
(24) Dangles, O.; Dufour, C. Flavonoid-protein interactions. In *Flavonoids: Chemistry, Biochemistry and Applications*; Andersen, Ø. M., Markham, K. R., Eds.; CRC Press: Boca Raton, FL, 2006; p 443.
(25) Soares, S.; Mateus, N.; de Freitas, V. Interaction of different polyphenols with bovine serum albumin (BSA) and human salivary α-amylase (HSA) by fluorescence quenching. *J. Agric. Food Chem.* **2007**, *55*, 6726−6735.
(26) Pastukhov, A. V.; Levchenko, L. A.; Sadkov, A. P. Spectroscopic study on binding of rutin to human serum albumin. *J. Mol. Struct.* **2007**, *842*, 60−66.
(27) Jurasekova, Z.; Marconi, G.; Sanchez-Cortes, S.; Torreggiani, A. Spectroscopic and molecular modeling studies on the binding of the flavonoid luteolin and human serum albumin. *Biopolymers* **2009**, *91*, 917−927.
(28) Xiao, J. B.; Zhao, Y. R.; Wang, H.; Yuan, Y. M.; Yang, F.; Zhang, C.; Yamamoto, K. Noncovalent interaction of dietary polyphenols with common human plasma proteins. *J. Agric. Food Chem.* **2011**, *59*, 10747−10754.
(29) Khan, M. K.; Rakotomanomana, N.; Dufour, C.; Dangles, O. Binding of citrus flavanones and their glucuronides and chalcones to human serum albumin. *Food Funct.* **2011**, *2*, 617−626.
(30) Dufour, C.; Dangles, O. Flavonoid-serum albumin complexation: determination of binding constants and binding sites by fluorescence spectroscopy. *Biochim. Biophys. Acta−Gen. Subj.* **2005**, *1721*, 164−173.
(31) Manzini, G.; Ciana, A.; Crescenzi, V. The interaction of serum albumins with various drugs in aqueous solution: Ggel permeation, calorimetric, and fluorescence data. *Biophys. Chem.* **1979**, *10*, 389−396.
(32) Lakowicz, J. R. *Principles of Fluorescence Spectroscopy*, 3rd ed.; Springer Science+Business Media: New York, 2006.
(33) Greenfield, N. J. Using circular dichroism spectra to estimate protein secondary structure. *Nat. Protoc.* **2006**, *1*, 2876−2890.
(34) Bi, S. Y.; Ding, L.; Tian, Y.; Song, D. Q.; Zhou, X.; Liu, X.; Zhang, H. Q. Investigation of the interaction between flavonoids and human serum albumin. *J. Mol. Struct.* **2004**, *703*, 37−45.
(35) Kratochwil, N. A.; Huber, W.; Müller, F.; Kansy, M.; Gerber, P. R. Predicting plasma protein binding of drugs: a new approach. *Biochem. Pharmacol.* **2002**, *64*, 1355−1374.
(36) Vuignier, K.; Schappler, J.; Veuthey, J.-L.; Carrupt, P.-A.; Martel, S. Drug-protein binding: a critical review of analytical tools. *Anal. Bioanal. Chem.* **2010**, *398*, 53−66.
(37) Seedher, N.; Agarwal, P. Complexation of fluoroquinolone antibiotics with human serum albumin: a fluorescence quenching study. *J. Lumin.* **2010**, *130*, 1841−1848.
(38) Abou-Zied, O. K.; Al-Lawatia, N. Exploring the drug-binding site Sudlow I of human serum albumin: the role of water and Trp214 in molecular recognition and ligand binding. *ChemPhysChem* **2011**, *12*, 270−274.
(39) Brodersen, R.; Sjödin, T.; Sjöholm, I. Independent binding of ligands to human serum albumin. *J. Biol. Chem.* **1977**, *252*, 5067−5072.
(40) Weber, G.; Daniel, E. Cooperative effects in binding by bovine serum albumin. II. The binding of 1-anilino-8-naphthalenesulfonate. Polarization of the ligand fluorescence and quenching of the protein fluorescence. *Biochemistry* **1966**, *5*, 1900−1907.
(41) Stryer, L. The interaction of a naphthalene dye with apomyoglobin and apohemoglobin: a fluorescent probe of non-polar binding sites. *J. Mol. Biol.* **1965**, *13*, 482−495.
(42) Cattoni, D. I.; Kaufman, S. B.; Flecha, F. L. G. Kinetics and thermodynamics of the interaction of 1-anilino-naphthalene-8-sulfonate with proteins. *Biochim. Biophys. Acta−Proteins Proteomics* **2009**, *1794*, 1700−1708.
(43) González-Béjar, M.; Alarcón, E.; Poblete, H.; Scaiano, J. C.; Pérez-Prieto, J. Stereoselective interaction of epimeric naproxen-RGD peptides with human serum albumin. *Biomacromolecules* **2010**, *11*, 2255−2260.
(44) Erlund, I.; Meririnne, E.; Alfthan, G.; Aro, A. Plasma kinetics and urinary excretion of the flavanones naringenin and hesperetin in humans after ingestion of orange juice and grapefruit juice. *J. Nutr.* **2001**, *131*, 235−241.
(45) Pandey, K. B.; Rizvi, S. I. Current understanding of dietary polyphenols and their role in health and disease. *Curr. Nutr. Food Sci.* **2009**, *5*, 249−263.
(46) D'Archivio, M.; Filesi, C.; di Benedetto, R.; Gargiulo, R.; Giovannini, C.; Masella, R. Polyphenols, dietary sources and bioavailability. *Ann. Ist. Super. Sanita* **2007**, *43*, 348−361.
(47) Nielsen, I. L. F.; Chee, W. S. S.; Poulsen, L.; Offord-Cavin, E.; Rasmussen, S. E.; Frederiksen, H.; Enslen, M.; Barron, D.; Horcajada, M.-N.; Williamson, G. Bioavailability is improved by enzymatic modification of the citrus flavonoid hesperidin in humans: a randomized, double-blind, crossover trial. *J. Nutr.* **2006**, *136*, 404−408.
(48) Gardana, C.; Guarnieri, S.; Riso, P.; Simonetti, P.; Porrini, M. Flavanone plasma pharmacokinetics from blood orange juice in human subjects. *Br. J. Nutr.* **2007**, *98*, 165−172.
(49) Boulton, D. W.; Walle, U. K.; Walle, T. Extensive binding of the bioflavonoid quercetin to human plasma proteins. *J. Pharm. Pharmacol.* **1998**, *50*, 243−249.
(50) Lucek, R. W.; Coutinho, C. B. The role of substituents in the hydrophobic binding of the 1,4-benzodiazepines by human plasma proteins. *Mol. Pharmacol.* **1976**, *12*, 612−619.

(51) McNamara, P. J.; Trueb, V.; Stoeckel, K. Ceftriaxone binding to human serum albumin: indirect displacement by probenecid and diazepam. *Biochem. Pharmacol.* **1990**, *40*, 1247−1253.
(52) Fehske, K. J.; Schläfer, U.; Wollert, U.; Müller, W. E. Characterization of an important drug binding area on human serum albumin including the high-affinity binding sites of warfarin and azapropazone. *Mol. Pharmacol.* **1982**, *21*, 387−393.
(53) Carter, D. C.; Ho, J. X. Structure of serum albumin. *Adv. Protein Chem.* **1994**, *45*, 153−203.
(54) Daneshgar, P.; Moosavi-Movahedi, A. A.; Norouzi, P.; Ganjali, M. R.; Madadkar-Sobhani, A.; Saboury, A. A. Molecular interaction of human serum albumin with paracetamol: spectroscopic and molecular modeling studies. *Int. J. Biol. Macromol.* **2009**, *45*, 129−134.
(55) Xiao, J. B.; Kai, G. Y. A review of dietary polyphenol-plasma protein interactions: characterization, influence on the bioactivity, and structure-affinity relationship. *Crit. Rev. Food Sci. Nutr.* **2012**, *52*, 85−101.
(56) Rolo-Naranjo, A.; Codorniu-Hernández, E.; Ferro, N. Quantum chemical associations ligand-residue: their role to predict flavonoid binding sites in proteins. *J. Chem. Inf. Model.* **2010**, *50*, 924−933.
(57) Nijveldt, R. J.; van Nood, E.; van Hoorn, D. EC.; Boelens, P. G.; van Norren, K.; van Leeuwen, P. A. M. Flavonoids: a review of probable mechanisms of action and potential applications. *Am. J. Clin. Nutr.* **2001**, *74*, 418−425.
(58) Manach, C.; Scalbert, A.; Morand, C.; Rémésy, C.; Jiménez, L. Polyphenols: food sources and bioavailability. *Am. J. Clin. Nutr.* **2004**, *79*, 727−747.
(59) Bandyopadhyay, P.; Ghosh, A. K.; Ghosh, C. Recent developments on polyphenol-protein interactions: effects on tea and coffee taste, antioxidant properties and the digestive system. *Food Funct.* **2012**, *3*, 592−605.
(60) Kroon, P. A.; Clifford, M. N.; Crozier, A.; Day, A. J.; Donovan, J. L.; Manach, C.; Williamson, G. How should we assess the effects of exposure to dietary polyphenols in vitro? *Am. J. Clin. Nutr.* **2004**, *80*, 15−21.
(61) Dangles, O.; Dufour, C.; Bret, S. Flavonol-serum albumin complexation. Two-electron oxidation of flavonols and their complexes with serum albumin. *J. Chem. Soc., Perkin Trans. 2* **1999**, *4*, 737−744.